Molecular Vision 2004; 10:821-31 <http://www.molvis.org/molvis/v10/a98>
Received 26 March 2004 | Accepted 18 October 2004 | Published 2 November 2004

©2004 Molecular Vision

Genetic correlations among texture characteristics in the human iris

Mats Larsson,[1] Nancy L. Pedersen[2]

[1]Center for Developmental Research, Department of Behavioral, Social, and Legal Sciences (BSR), Örebro University, Örebro, Sweden; [2]Department of Medical Epidemiology and Biostatistics, Karolinska Institute, Stockholm, Sweden

Purpose: To estimate the magnitude of genetic correlations among five general textural characteristics of the human iris.
Methods: Color photographs of iris were available from 100 monozygotic and 99 dizygotic twin pairs. Comparative scales were constructed based on ratings of the subjects' left iris. To explore the genetic and environmental covariation among frequency of Fuchs' crypts, frequency of pigment dots, iris color, the extension, and distinction of Wolfflin nodules, and contraction furrows, a structural equation model with Cholesky decomposition was applied to variance-covariance matrices for monozygotic (MZ) and dizygotic (DZ) pairs.
Results: Significant genetic correlations fell between -0.22 and 0.44 and accounted almost entirely for the phenotypic correlations among the iris characteristics. No evidence for individual specific environmental effects in common to the characteristics was found.
Conclusions: The modest genetic correlations indicate that there is little overlap in the genetic influence for these characteristics. Candidate genes with embryological and histological expression patterns in the eye could potentially influence the iris characteristics' variability.

Despite hundreds of molecular studies investigating genes that influence the health and function of the human iris, there are only few studies available that have evaluated the relative importance of genes for variation in iris textural qualities in normally developed eyes. In the few studies reported, the relative importance of genetic influences (heritability) on iris characteristics is substantial. The heritability for eye color in the Louisville Twin Study was 98% [1], whereas the heritability for Fuchs' crypts in the main stroma leaf, pigment dots, Wolfflin nodules, and contraction furrows in a German twin sample were, 66, 58, 78, and 78 percent, respectively [2]. There were no sex differences in heritability in these studies. The only iris characteristics for which heritability differs as a function of age are eye color and Wolfflin nodules, for which greater estimates were observed in the older cohorts. These findings suggest that iris characteristics in populations with normal eye development are moderately to highly heritable and generally show no sex specific genetic influences.

Potential candidate genes responsible for variation in iris texture characteristics are different alleles of *Pax6* and its downstream target genes [3], *COX-1*, *COX-2*, *VEGF*, *Ezrin*, *IR 185/OPTC*, *FKHL7/FOXC1*, *FOXC2*, *TIGR/GCL1A/Myocilin*, *RIEG1/PITX2*, *Lmx1b*, *Hox-7.1*, *Hox-8.1*, the *P* gene [4-17] as well as other genes that are expressed in the human iris [18,19]. Many of these genes influence more than one eye phenotype [20], which suggests that there may be pleiotropic effects on different textural characteristics in the iris. For instance, the *Pax6* gene may influence both the crypt frequency on the iris surface, and the extension and distinction of contraction furrows. *Pax6* is expressed both early [21] and late [4] in iris development. Family members with aniridia, which originates from *Pax6* deficiencies [20], have been observed with a broad spectrum of iris abnormalities, including abnormal crypt and contraction furrow structure [22]. One could therefore imagine that different alleles of *Pax6* could impact several aspects of the iris tissue in normally developed eyes. However, the extent to which there is overlap of genetic effects (i.e., a genetic correlation) among different iris characteristics is not known.

The purpose of this study is to estimate the genetic correlations among five general textural quality characteristics in the human iris. The genetic contributions to the observed phenotypic correlation among frequency of Fuchs' crypts in the main stroma leaf, frequency of pigment dots, iris color, the extension, and distinction of Wolfflin nodules as well as contraction furrows were examined in a sample of monozygotic (MZ) and dizygotic (DZ) twins.

METHODS

Sample: Data for this study came from a German sample of 100 monozygotic twin pairs reared together (54 male-male, 46 female-female), and 99 dizygotic pairs reared together (27 male-male, 33 female-female, 39 male-female) [23]. The mean age was 20.1 (5-70 years, SD=12.4), and 20.5 (4-72 years, SD=12.3), respectively. All were volunteers with good ocular health who were recruited through advertising in the town Braunschweig close to Hanover, Germany. The human subjects committee at Braunschweig University reviewed the research protocol. Black and white photographs were taken of

Correspondence to: Mats Larsson, Center for Developmental Research, Department of Behavioral, Social, and Legal Sciences (BSR), Örebro University, 701 82, Örebro, Sweden; Phone: (+46) 19 303415; FAX: (+46) 19 303484; email: mats.larsson@bsr.oru.se

the face (front and profile), mouth, eye area, nose, and ears, and close-up color photographs were taken of the subjects' iris.

Zygosity was determined by comparing intra-pair similarity for 10 physical characteristics of the head, including eye color, hair type, and shape of the ears. The attributes were selected on the basis of the diagnostic rules developed by Nichols and Bilbro, 1966 [24], which have been shown to predict zygosity as determined by red blood cell polymorphism analysis with at least 94% accuracy [25]. Two of the twin pairs who claimed to be monozygotic had too large intra-pair differences to be accepted by the algorithm and were excluded from the sample.

Material: A stereomicroscope (ZEISS-Universalspaltlampe 30 SL/M, Oberkochen, Germany) with an attached camera (Pentax 1000, Tokyo, Japan) with a 125 mm lens was used to obtain color photographs of the subjects' iris. The exposure time was <1/1000 s and set automatically by the flash exposure control. The shutter speed on the camera was set to 1/60 and the aperture was set to 32. To assist focus adjustment and to standardize the extent the iris was dilated, a lamp with the same voltage was shone into the subjects' iris during the time it took to adjust the focus of the lens and take the photos. All rolls of film used for the twins had the same charge number. Close-up color photos (where the diameter of the iris on the slide was about 22 mm) were taken of both irises from all subjects. The photo slides of the subjects' irises were placed on 12 CD-ROM discs. The quality of the transformation from slide positives to the images on the CD-ROM was chosen through Kodak's Photo-CD (5 levels, 3072

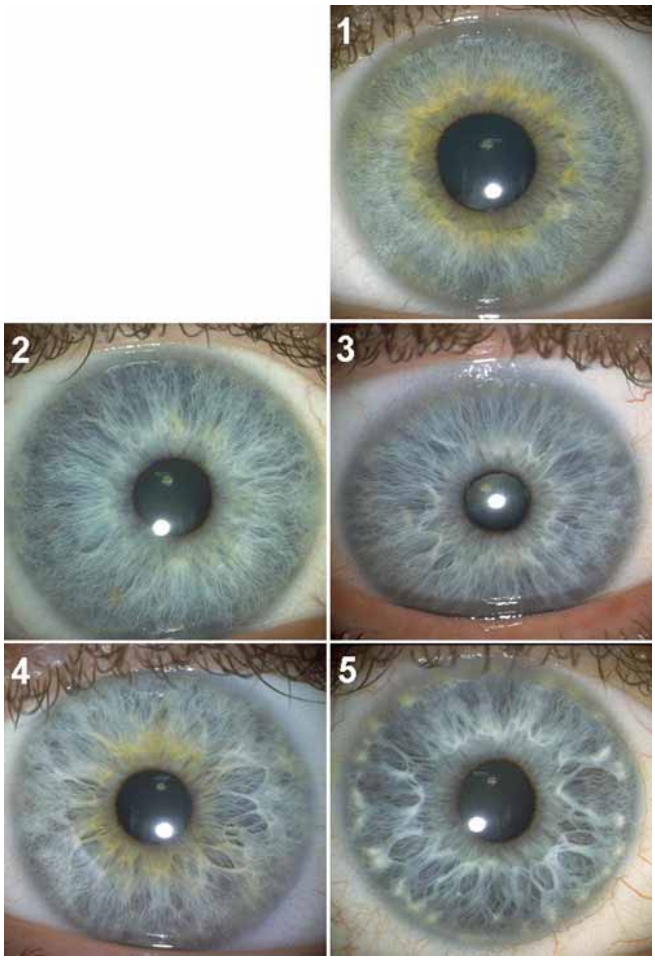

Figure 1. Frequency of Crypts. Photos 1-5 created a 5-point scale, which were used to measure the frequency of Fuchs' crypts. Photo 1 in the scale contains no Fuchs' crypts. The fibers lay parallel to each other and form a dense uniform tissue texture. Photo 2 was dense but compared to photo 1 was slightly more open in tissue texture. In photo 3, a minimum of 4 Fuchs' crypts in the main stroma leaf are clearly visible. In photo 4, the tissue texture was more permeable and the Fuchs' crypts are larger. In photo 5, Fuchs' crypts of different sizes cover nearly the entire iris spot.

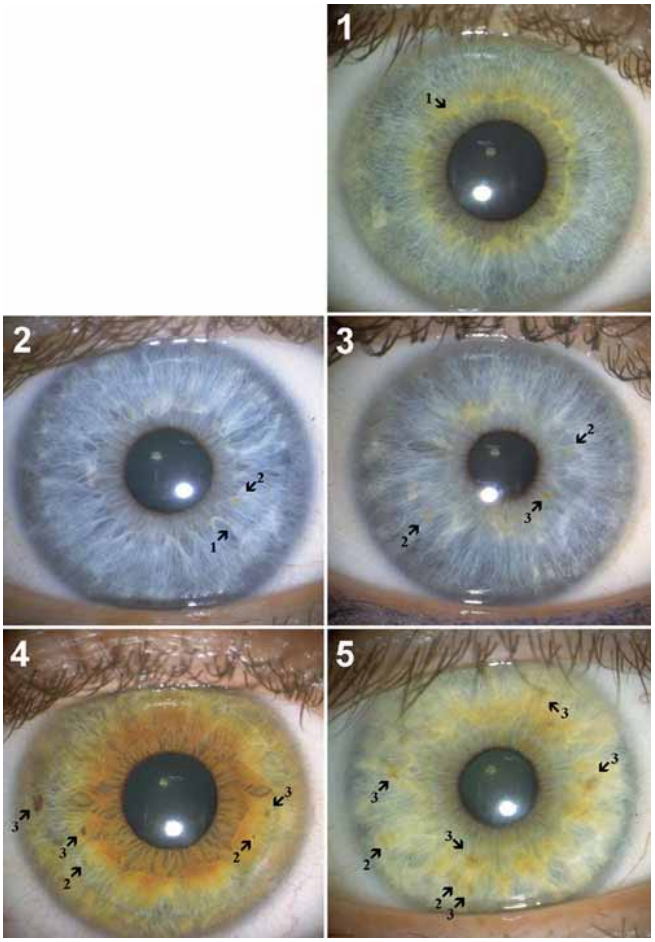

Figure 2. Frequency of Pigment Dots. A 5-point scale were used to measure the frequency of pigment dots. The numbered arrows that point towards different pigment dots illustrate the judgement categories of melanin accumulation. For example, melanin accumulations most similar to the pigment dots that have an arrow pointing towards it with the attached number 1, should be judged as category 1. Pigment dots with the attached number 2, should be judged as category 2 etc. Based on standardized rules of how many pigment dot classified for each category, the most appropriate scale step for each subject were determined. Raters judged all melanin accumulations visible on the iris photo.

x 2048 pixels; Kodak, Rochester, New York, USA). The photos were viewed on a high contrast color computer screen (Model: FlexScan F55; Eizo, Ishikawa, Japan) with 1024 x 768/85 Hz resolution (0.28 mm Dot Pitch CRT; fH:27-70 kHz/ fV: 50-120 Hz) using the software program PhotoShop 4.0. Iris photographs and other characteristics of the sample were purchased from Dr. Angelica Burkhardt, Institute for Human Biology, Technical University Carolo-Wilhelmina in Brunswick, Germany.

The first author constructed five continuous scales, one for each iris characteristic of interest. The pictures used for the scales may be seen in Figure 1 for the frequency of crypts, Figure 2 for the frequency of pigment dots, Figure 3 for iris color, Figure 4 for the frequency of Wolfflin nodules, and Figure 5 for contraction furrows. Two independent raters, blind to zygosity, graded the photos of the subject's iris characteristics using the reference photos. The raters' judgments were scored as continuous variables. Scale construction, the rating procedure, and results of the reliability test of the procedures are reported in detail in Larsson et al. [2].

Quantitative genetic models: Monozygotic twins share in principle all of their genes, while dizygotic twins share, on average, half of their segregating genes. By comparing how similar monozygotic and dizygotic twin pairs are on the iris characteristics of interest, one can assess to what extent genetic and environmental factors contribute to within pair covariances. Quantitative genetic methods subdivide genetic influences into additive and nonadditive components [26]. The distinction refers to the way in which alleles co-act to influence expression of the phenotype: The additive component reflects the summed effects of alleles within and across loci, and the nonadditive component reflects the interaction of alleles within (dominance) and across (epistasis) different loci. Environmental influences may also be important for individual differences and are typically subdivided into nonshared, and shared components. Nonshared environmental influences are unique to each individual and therefore contribute only to differences within twin pairs, regardless of their genetic similarity. Errors of measurement, which contribute to twin differences, are included in the nonshared environmental component. Shared environmental components, such as family environments, make members of a twin pair similar regardless of their genetic similarity. If genetic influences are important for a trait, MZ correlations should be approximately twice the magnitude of DZ correlations. Analogous comparisons can be made to evaluate sources of covariation among the traits. We distinguish between the "twin correlation", which is the within pair correlation for a single scale (e.g., correlation of Twin 1's crypt score with Twin 2's crypt score), and the cross-

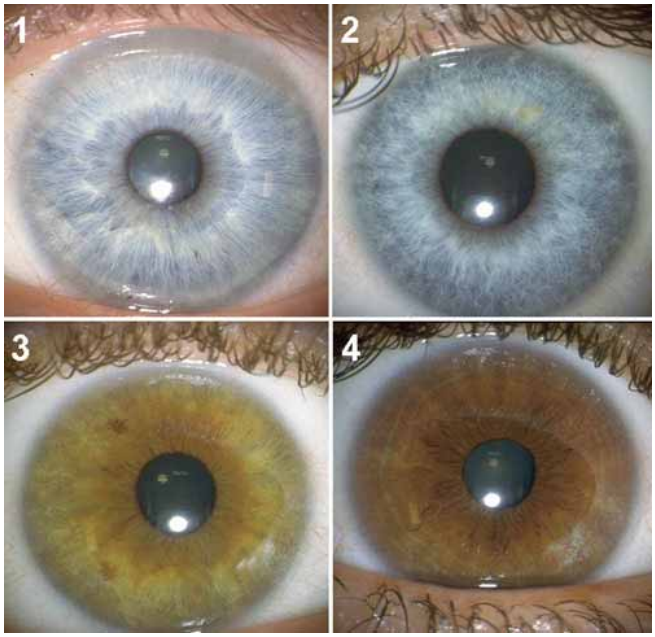

Figure 3. Iris color. Photos 1-4 created a 4-point scale, which was used to measure iris color. The color of the iris in photos 1, 2, 3 and 4 are gray, blue, hazel, and brown, respectively.

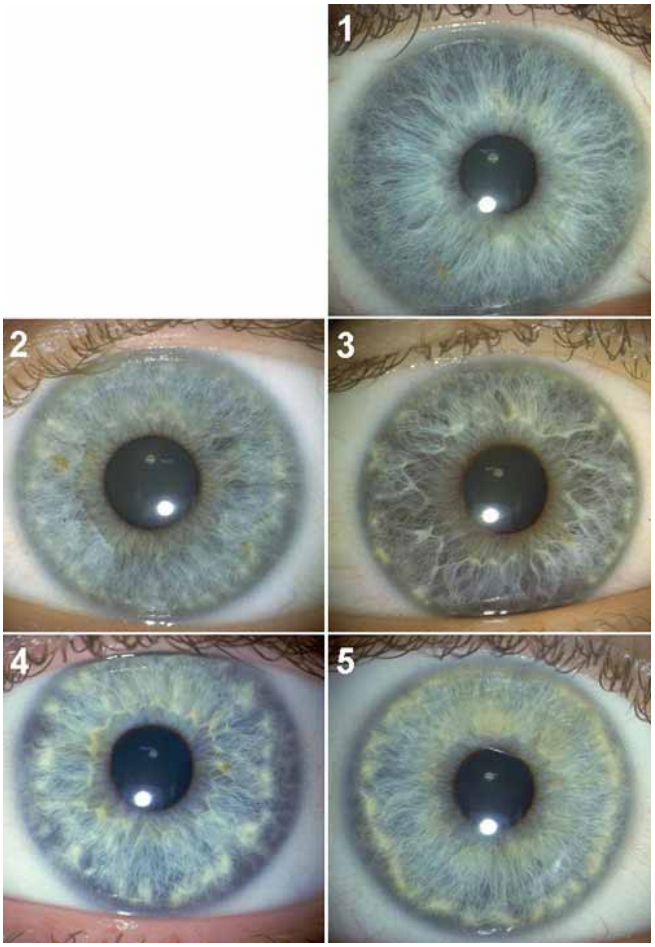

Figure 4. Wolfflin Nodules. Photo 1 in the scale has no Wolfflin nodules at the periphery of the iris. In photo 2, a ring of clumped nodules extends from 3 to 10 o'clock. In photo 3, the white nodules are more visible and distinct from each other. In photo 4, the nodules lager, are lighter and are closer together. In photo 5, the Wolfflin nodules have formed a uniform white ring that is much thicker and distinct than in the previous scale steps. A corresponding scale, showing what the Wolfflin nodules look like when partly covered by pigment was used to assist the raters judgments.

twin correlation, which is the correlation within a twin pair across two scales (e.g., correlation of Twin 1's crypt score with Twin 2's pigment dots score). Thus, if genetic influences are important for the covariation between two traits, the MZ cross correlation should be twice as large as the DZ cross correlation.

Recent univariate analyses based on this sample [2] demonstrated that genetic influences for all iris characteristics except Wolfflin nodules were additive and therefore we chose to test models with additive genetic effects (h^2). The quantitative genetic expectations for the covariances among the multiple measures (assuming additivity of genetic effects) are 1.0 and 0.5 for monozygotic and dizygotic twin pairs, respectively [26].

Associations among the iris characteristics were evaluated using a Cholesky decomposition model, as depicted in Figure 6. For simplicity, the diagram shows sources of variance for only one twin and excludes shared environmental influences. Each of the five measures of iris characteristics loaded on latent additive genetic (A_1 through A_5) and environmental factors (E_1 through E_5). All five scales load on the first genetic and environmental factors. The second latent factor is orthogonal to the first factor and has loadings on the subsequent four scales. The third and fourth latent factors operate in the same manner, reflecting influences independent of the prior factors. The fifth latent factor is unique to the contraction furrow scale. Using this model, the genetic and environmental etiology of the relationships among iris characteristics can be assessed (i.e., the extent to which the correlations among the measures are due to genetic and environmental influences). In addition, estimates genetic and environmental correlations among the measures can be computed.

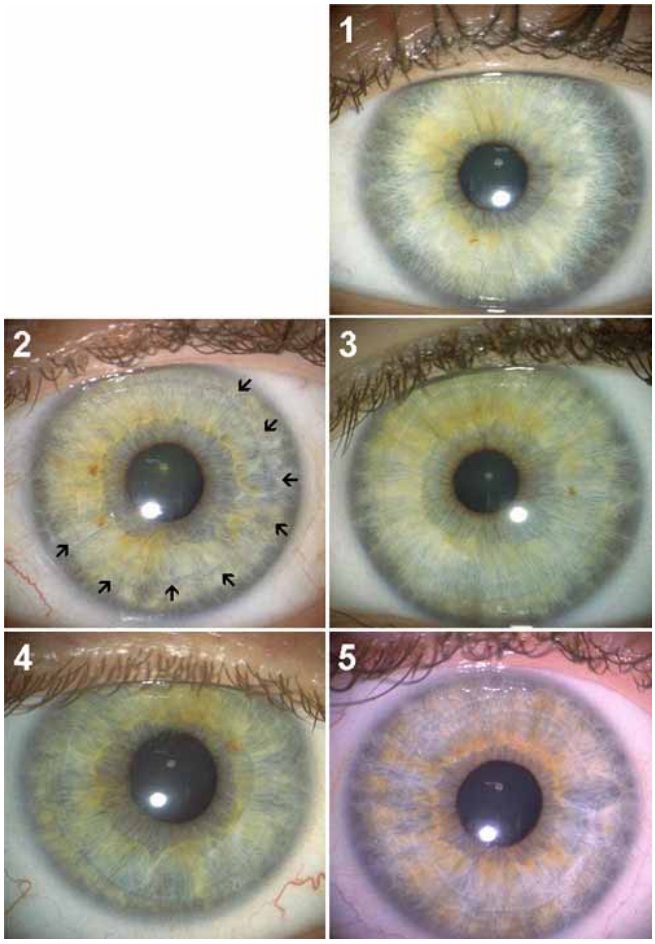

Figure 5. Contraction Furrows. This scale measured the extension and distinction of contraction furrows in the main stroma leaf of the iris. Photo 1 in the scale had no contraction furrows. In photo 2, a contraction furrow extends halfway from the periphery of the iris from 1 to 8 o clock. In photo 3, the contraction furrows are more distinct and extend around the whole iris. In photo 4, the contraction furrows are more distinct. In photo 5, a minimum of two full circles of contraction furrows present. A corresponding scale showing what the contraction furrows look like in brown colored iris were also used to assist the rater judgments.

The genetic correlation (r_A), which can range from -1.00 to 1.00, is an estimate of the extent to which the same genes influence two variables, reflecting the degree of pleiotropy. Estimates of genetic and environmental correlations among the iris characteristics are obtained from the standardized path coefficients. For example, the product of the paths a_{11} and a_{12} estimates the phenotypically standardized genetic covariance:

$$h_{11} r_A h_{12}$$

where h is the square root of the heritability of the indicated measure and r_A is the genetic correlation between the two measures. The phenotypically standardized genotypic covariance represents the genetic component of the phenotypic correlation (r_p). Similarly, $e_{11}e_{12}$ represents the environmental component, so:

$$r_P = a_{11}a_{12} + e_{11}e_{12}$$

The genetic correlation is calculated by dividing the phenotypically standardized genetic covariance with the product of the square roots of the two heritabilities:

$$r_A = \frac{h_{11} r_A h_{12}}{h_{11} h_{12}}$$

The environmental correlation is computed in an analogous fashion.

A full model and three nested models were tested [26]. The first model estimated additive genetic, shared environmental, and nonshared environmental parameters freely. The

second was like the first except that the potential contribution from all parameters representing shared environmental effects were fixed at 0, testing whether shared environmental effects were significant. The third model was like the second except that the 10 additive genetic parameters representing genetic covariation (a_{12}, a_{13}, a_{14}, a_{15}, a_{23}, a_{24}, a_{25}, a_{34}, a_{35}, and a_{45}) were also fixed at 0, testing whether the genetic influences on the iris characteristics were independent of each other. In other words if this model fit well, there is no genetic covariation and genetic influences do not contribute to the phenotypic correlation. The fourth model was like the second except that the 10 nonshared environmental parameters (e_{12}, e_{13}, e_{14}, e_{15}, e_{23}, e_{24}, e_{25}, e_{34}, e_{35}, and e_{45}) were fixed at 0, testing whether the environmental influences on the iris characteristics were independent of each other.

In order to remove variance caused by the effects of gender and age in the twin analyses, scores for all twins with complete data on the five iris characteristics (n=398) were adjusted for gender, age and gender by age using the regression procedure described by McGue and Bouchard [27]. All five scales were positively skewed, and for this reason the scores were log transformed. Model fitting analyses using Mx [28] were based on observed variance and covariance matrices computed separately for MZ and DZ twin pairs using SPSS [29]. Choice of the best fitting model was based on the Akaike information criterion (AIC) [30], which equals the χ^2 statistic minus twice the degrees of freedom (df):

$$AIC = \chi^2 - 2df$$

This reflects both the goodness of fit and parsimony of the model. The model with the most negative value for the AIC was considered the best model.

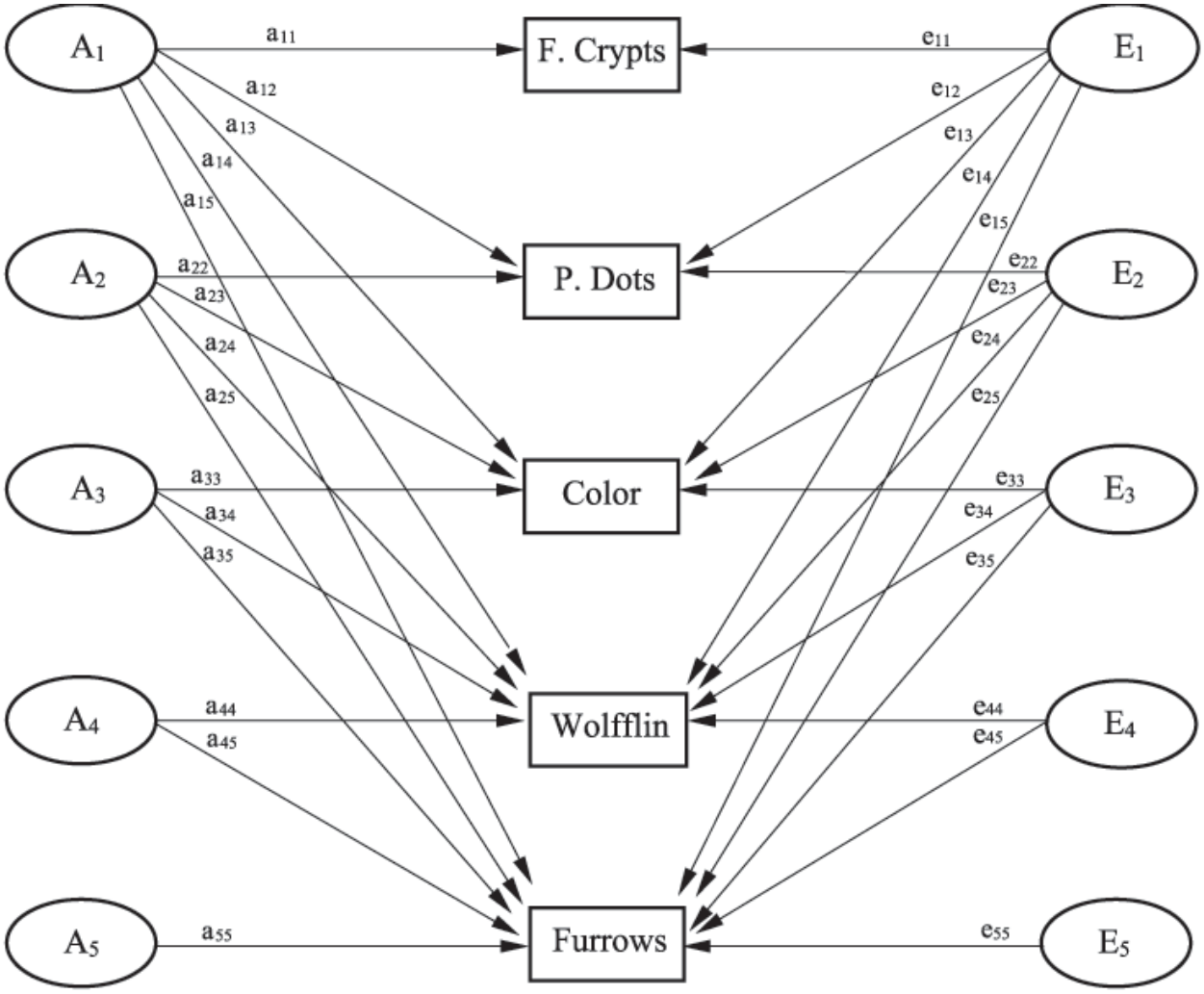

Figure 6. The factor structure underlying the five iris characteristics. This illustrates the genetic and environmental factor structures for the five iris characteristics Fuchs' crypt frequency (Crypts), pigment dot frequency (P. Dots), iris color (Color), extension and distinction of Wolfflin nodules (Wolfflin), and Contraction furrows (Furrows) for one twin only. Each of the five measures of iris characteristics loaded on additive genetic (A_1 through A_5) and environmental latent factors (E_1 through E_5).

RESULTS

Descriptive statistics: Table 1 shows the means and standard deviations for the five iris characteristics of interest in MZ and DZ twins. Levene's Test for Equality of Variances and t-tests were carried out to examine mean and variance differences between the two groups. Two of the five scales showed no significant mean or variance differences between the groups, satisfying a basic assumption of the twin method. Variance differences can affect the fit of the models. However, the full model received an acceptable fit (Table 2), indicating that the magnitude of the variance differences was too small to obscure the fit to any great extent.

Age was significantly associated with increasing number of pigment dots (r=0.31, p<0.05), Fuchs' crypts (r=0.14, p<0.05), as well as lighter iris color (r=-0.14, p<0.05), and less distinct contraction furrows (r=-0.12, p<0.05). Males had a greater number of Fuchs' crypts than females ($t_{(396)}$=-2.17, p<0.05).

Phenotypic correlations: The phenotypic correlations among the iris characteristics are presented in Table 3. Six out of ten phenotypic correlations were significant. Darker iris color, lower frequency of Fuchs' crypts, and increasing frequency of pigment dots were associated with more extended and distinct contraction furrows. Increasing number of pigment dots was also associated with darker iris color. Increasing number of Fuchs' crypts and lighter iris color were associated with more extended and distinct Wolfflin nodules. All other correlations were non significant and lower than 0.10.

The twin correlations and cross correlations for the five iris characteristics, separately for MZ and DZ twin pairs, are reported in Table 4.

The MZ twin correlations were higher than the DZ twin correlations, providing support for substantial genetic influences as reported previously [2]. The MZ cross correlations were in most cases greater than the corresponding DZ cross correlations, at least for the pairs of measures for which the phenotypic correlation was significant. This pattern of twin cross correlations suggests that the covariance among the five iris characteristics is determined largely by genetic influences shared by the measures.

Model fitting analysis: Table 2 summarizes goodness of fit statistics for the full Cholesky Model and the three submodels. Two main findings emerged from these analyses. First, shared environmental effects were absent and could be constrained to 0 without a deterioration of the fit to the data ($\Delta\chi^2$=6.94, df=15, p=0.96). In fact Model 2 (excluding shared environmental factors) yielded a better fit than Model 1 (AIC=-77.18 versus -54.12). Second, the additive genetic factors were important for covariation among the five iris characteristics,

Table 1. Means and standard deviations for five scales describing iris characteristics in monozygotic and dizygotic twins.

	Monozygotic (100 pairs)		Dizygotic (99 pairs)	
Scales	Mean	SD	Mean	SD
Crypts	2.14	0.90	2.20	0.88
P. dots*	2.03	1.04	1.76	0.98
Color**	2.32	0.90	2.16	0.78
Wolfflin	1.40	0.67	1.45	0.77
Furrows*	2.25	1.18	1.85	1.11

Asterisk indicates the significant mean differences between monozygotic and dizygotic twins (p<0.05). Double asterisks indicates the significant variance differences between monozygotic and dizygotic twins (p<0.05).

Table 2. Goodness of fit statistics for the full Cholesky Model and three nested submodels

Models	chi-sq	df	p	AIC
Full model	75.88	65	0.18	-54.12
No shared environmental effects	82.82	80	0.39	-77.18
No genetic correlations	197.51	90	0.00	17.51
No environmental correlations	92.77	90	0.40	-87.23

Goodness of fit statistics for the full Cholesky model and three nested submodels in which all parameters in common to the iris characteristics (e.g. a_{12}, a_{13}, a_{14}, a_{15}, a_{23}, a_{24}, a_{25}, a_{34}, a_{35}, a_{45}) are fixed at zero. The table lists the χ^2 statistic (chi-sq), the degrees of freedom (df), the estimated significance level (p; if p<0.05 then the model does not fit), and the Akaike information criterion (AIC). The model with the most negative value for the AIC was considered the best model.

Table 3. Phenotypic correlations among the measures of the five iris characteristics

Scales	Crypts	P. Dots	Color	Wolfflin	Furrows
Crypts	-				
P. dots	0.00	-			
Color	0.03	0.13*	-		
Wolfflin	0.22*	0.02	-0.19*	-	
Furrows	-0.29*	0.13*	0.39*	-0.06	-

The asterisk represents a p<0.05 (by a two tailed test).

Table 4. Twin correlations and twin cross correlations for the five iris characteristics by zygosity

	Monozygotic twins (100 pairs)				
Scales	Crypts	P. Dots	Color	Wolfflin	Furrows
Crypts	0.66*				
P. dots	-0.05	0.58*			
Color	0.06	0.20*	0.87*		
Wolfflin	0.22*	-0.05	-0.18	0.75*	
Furrows	-0.23*	0.24*	0.37*	0.03	0.79*

	Dizygotic twins (99 pairs)				
Scales	Crypts	P. Dots	Color	Wolfflin	Furrows
Crypts	0.34*				
P. dots	-0.12	0.27*			
Color	0.06	0.25*	0.53*		
Wolfflin	-0.10	-0.10	-0.06	-0.20*	
Furrows	-0.16	0.10	0.38*	-0.17	-0.28*

Within pair correlations are shown on the diagonal, and the cross-twin correlations are shown off-diagonal. The asterisk represents a p<0.05 (by a two tailed test).

whereas the nonshared environmental factors were not. Thus, Model 4 provided the most parsimonious description of the relationships among the five iris characteristics. Nevertheless, we chose to present the results based on Model 2, as they provide important information about nonshared environmental influences for the individual measures. The maximum likelihood parameter estimates from Model 2 are presented in Table 5. The standardized path coefficients and the 95% upper and lower confidence intervals of the estimates within parenthesis after each estimate from Model 2 are depicted in the Cholesky Model (Figure 7).

The genetic covariances in Table 5 were very similar to the corresponding phenotypic correlations, indicating that the genetic influences accounted almost entirely for the phenotypic correlations among the five iris characteristics. The significant genetic correlations ranged from -0.22 to 0.44.

Because pigment dots generally develop before adulthood and then show little change over time [31,32], we also performed analyses (data not shown) excluding twins under 15 years of age. In these analyses the phenotypic correlations between pigment dots and the other iris characteristics were negligible and none of the genetic correlations with pigment dots reached significance. The remaining correlations were almost identical to those in the full sample.

DISCUSSION

The purpose of the present study was to estimate the genetic correlations among five iris characteristics: frequency of Fuchs' crypts; frequency of pigment dots; iris color; extension and distinction of Wolfflin nodules; and contraction furrows. Genetic correlations ranged between -0.22 and 0.44. No evidence for significant environmental covariation was found. Structural equation models demonstrated that the phenotypic correlations among the iris characteristics were due to genetic covariation.

Table 5. Maximum likelihood parameter estimates from Model 2, excluding shared environmental influences

	Genetic				
Scales	Crypts	P. Dots	Color	Wolfflin	Furrows
Crypts	0.66*				
P. Dots	-0.06	0.56*			
Color	0.06	0.24*	0.84*		
Wolfflin	0.37*	0.00	-0.22*	0.76*	
Furrows	-0.41*	0.24*	0.44*	-0.05	0.77*

	Environmental				
Scales	Crypts	P. Dots	Color	Wolfflin	Furrows
Crypts	0.34*				
P. Dots	0.08	0.44*			
Color	-0.04	-0.13	0.16*		
Wolfflin	-0.13	0.07	-0.05	0.24*	
Furrows	0.01	-0.09	0.17	-0.12	0.23*

Diagonal elements are the heritabilities and environmentalities, elements below are the genetic and environmental correlations. The asterisk represents a $p<0.05$ (by a two tailed test).

The significant genetic correlations were relatively few and low in magnitude, which may not be surprising considering morphological differences during development. One such difference is the timing of formation. For instance, Fuchs' crypts are patch like atrophies of the anterior border layer. The principal distribution and depth of these atrophies are present at birth [33]. Pigment dots on the other hand, rarely appear on the surface of the anterior border layer before the age of six [31]. The genetic correlation between Fuchs' crypts and pigment dots is close to zero (r_A=-0.06, *ns*), in keeping with this developmental difference. Similarly, no genetic correlation could be found between Fuchs' crypts and iris color (r_A=0.06, *ns*). The melanocytes, which determine iris color [34], normally reach their genetically determined amount of melanin in early childhood and then usually remain constant in adulthood [1]. These results suggest that morphological differences during development, in this case the timing in the formation of iris characteristics, tend to preclude a potential genetic correlation. Similarly, iris characteristics that originate from different processes within the cells generally do not share any genetic factors in common. Thus, Wolfflin nodules, which are accumulations of fibrous tissue in the anterior border layer [35,36], did not share any genetic influences with pigment dots (r_A=0.00, *ns*).

An examination of morphology for iris characteristics with significant genetic correlations suggests that those originating from the same cell layers, or cell layers that are likely to contribute to an iris characteristic's prevalence, generally do share genetic factors. For instance, contraction furrows become manifest due to a tendency of the iris to fold in the same location when the iris aperture adapts to different light conditions. Contraction furrows may therefore be influenced by the overall thickness and density of the iris, which implies that all five cell layers in the iris i.e., the anterior border layer, stroma, dilator muscle fibers and the anterior and posterior epithelial layers, potentially could influence the extension and distinction of contraction furrows. It is therefore not surprising that all iris characteristics measured in the anterior border layer except Wolfflin nodules, i.e., Fuchs' crypts, pigment dots and iris color, shared significant genetic correlations with contraction furrows. The strongest of these was iris color, for which the genetic influences contributing to more pigmented iris also contributed to increased extension and distinction of contraction furrows (r_A=0.44, $p<0.05$). This finding, which suggests that the amount of melanin in the anterior border layer influences the overall density and thickness of the iris, is supported by previous published results. Imesch et al. [34] found that the number of melanosomes and the area they cover in the melanocyte's cytoplasm in hazel and brown iris were three to five times as large as in blue iris. Thus, genes involved in the differentiation of melanocytes and melanin production may contribute to the genetic correlation between iris color and contraction furrows. The gene *Mitf* is required for the differentiation of melanocytes as well as the onset and maintenance of melanin production in these cells [37-39]. Moreover, several mutations of the tyrosinase gene *TYR* and the *P* gene produce clinical albino phenotypes [18]. Recent linkage findings

suggest that much of the genetic variance for eye color in normally developed eyes is explained by the *P* gene [14]. Thus, *Mitf*, *TYR*, and the *P* are candidate genes for explaining some of the genetic correlation between iris color and the extension and distinction of contraction furrows.

The second strongest genetic correlation was between fewer Fuchs' crypts and more extended contraction furrows (r_A=-0.41, p<0.05). Increasing number of Fuchs' crypts decreases the overall density and thickness of the iris and this may allow the iris to fold in different locations when the pupil adapts to different light conditions. This, in turn, would give less extended and distinct contraction furrows. Alternatively, contraction furrows may still be present in the deeper cell layers of irises with high crypt frequency, but due to the patch like absence of tissue in the anterior border layer, leave less extended contraction furrows there.

In turning to the task of identifying plausible candidate genes that could explain this finding, the embryological and histological development of Fuchs' crypts needs to be considered. Fuchs' crypts may represent local anomalies in the embryonic pupillary membrane where tissue fails to form because of the lack of inductive signals occurring sometime between the third and six month of gestation. By the seventh month of gestation, the absorption of the embryonic pupillary membrane is complete and could spill over into the main stroma leaf [33]. Genes expressed in precursors to the anterior border layer and underlying stroma during this period can thus be considered to be candidate genes for crypt frequency. However, due to the interdependence of the variability of Fuchs' crypt and contraction furrows mentioned earlier, such genes could also be considered to be candidate genes for the covariation between Fuchs' crypts and contraction furrows.

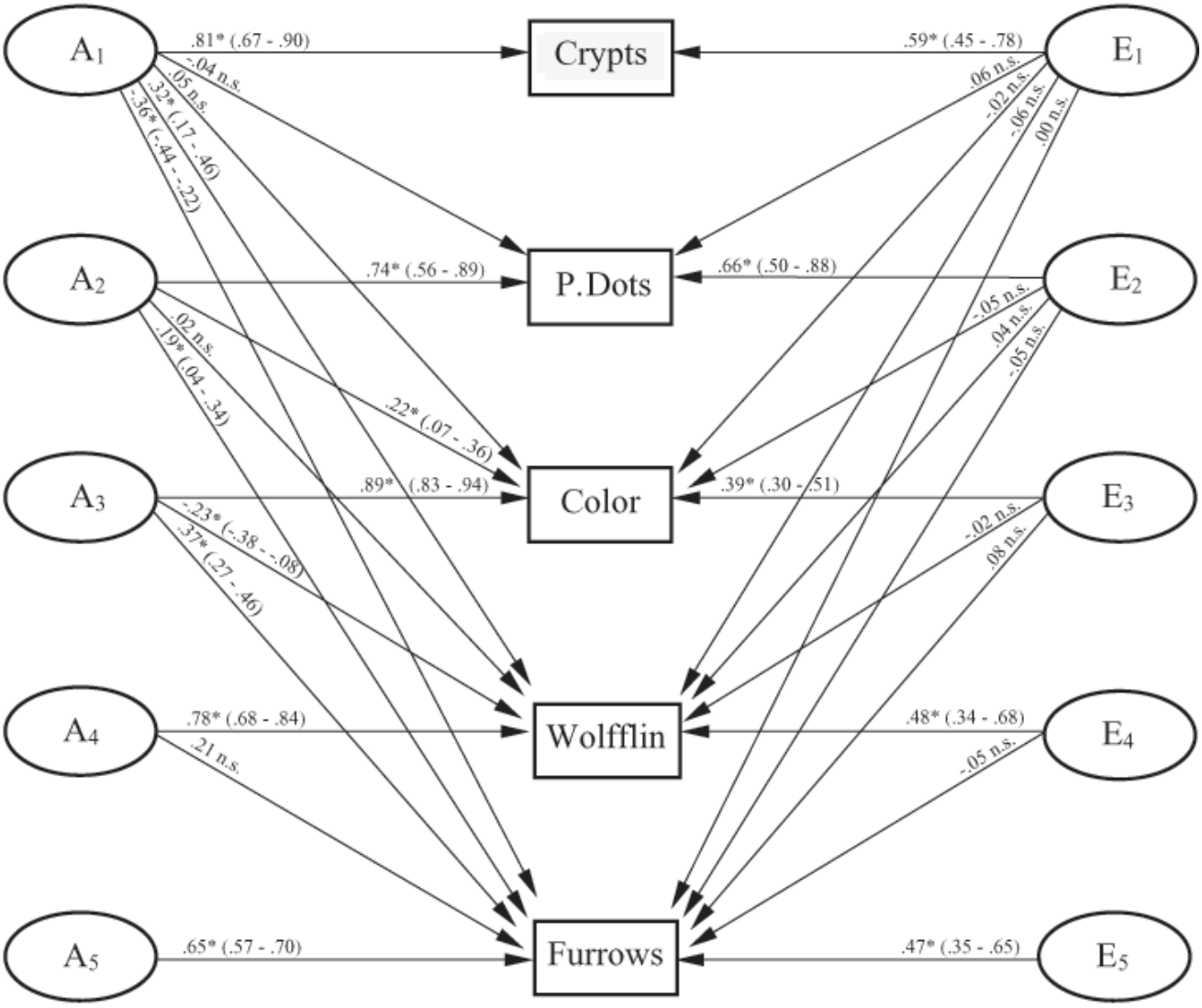

Figure 7. Standardized path coefficients and 95% confidence intervals from Model 2. All paths representing additive genetic and nonshared environmental effects were freely estimated. Shared environmental effects were fixed at 0. Statistically significant (p<0.05; based on a chi-square with 1 df) differences are marked with an asterisk.

The gene *Mitf*, implicated in the development of melanocytes in the anterior border layer, is an obvious candidate gene for the genetic correlation between crypt frequency and contraction furrows. But *Mitf* also negatively regulates the expression of *Pax6* [40], a master control gene for iris development, and decreases or increases over the normal level of *Pax6* expression lead to specific eye anterior segment defects [41]. The genetic correlation between crypt frequency and contraction furrows may therefore be dependent on genes that interact with *Pax6* (such as *Mitf*) and downstream targets of *Pax6*, such as *Six3* as well as *Lmx1b*, *Hox-7.1*, and *Hox-8*. These are expressed in a subset of periocular mesenchymal cells originating from the neural crest, which during morphogenesis migrate from the optic cup margin over the lens to form the embryonic pupillary membrane. These, in turn, will develop to become the fibroblasts, melanocytes and collagen fibers (type I and III) in the adult iris [33]. Mis-expression of *Six3* in the chick attenuates proliferation and differentiation of periocular mesenchymal cells of the iris. This implies that *Six3*, *Lmx1b*, *Hox-7.1*, and *Hox-8*, may be involved in the formation of Fuchs' crypts in the anterior border layer [3,15-17]. Other genes that may influence the development of Fuchs' crypts as well as the variability of contraction furrows in the human iris are *RIEG1/PITX2* [12], and *FKHL7/FOXC1* [42].

The third strongest significant genetic correlation was between more extended rings of Wolfflin nodules and higher frequency of Fuchs' crypts (r_A=0.37, $p<0.05$). This may reflect observations that Wolfflin nodules, which mainly contain collagen fibers [35,43], in part are rest products from atrophy in the anterior border layer [44,45]. The histological similarity between Brushfield spots and Wolfflin nodules, as well as the fact that the position and the appearance of Brushfield spots for patients with Down's syndrome can be quite similar to what is seen in normal controls [35,43], may indicate that the region on chromosome 21 that has been associated with Brushfield spots [46] also holds candidates genes for Wolfflin nodules. The genes *ERG* [47], *ETS2* [48], *HMG* [49], *MX1* [50], *WRB* [51], *DSCR1* [52], and *SH3BGR* [53] as well as other genes which map to this region [54], could from this perspective be potential candidate genes for Wolfflin nodules and by extension, the genetic correlations between crypt frequency and Wolfflin nodules. However, normal individuals with mutations in some of those genes do not have Wolfflin Nodules or Brushfield spots, indicating that their appearance may depend on interactions between several genes. Research including both normal individuals with Wolfflin nodules and Down's syndrome patients with Brushfield spots needs to be performed to find out the extent to which the genetic origin of Wolfflin nodules differs from, or overlaps with, the genetic origin of Brushfield spots.

The differences in results for pigment dots in the full sample versus the sample excluding twins younger than 15 years old are difficult to explain, as we anticipated that the genetic correlations should have been greater in samples that have reached their full development of pigment dots. One likely explanation is that the sample size that remained lacked the power to detect correlations in the 0.10 range. Alternatively, there simply is little if any association between pigment dots and the other iris characteristics.

Methodological implication for molecular iris research: Given the high inter-rater reliabilities (91%-97%), heritabilities (58%-90%) [2] and relatively low but significant genetic correlations (0.22 to 0.44) for the iris characteristics reported, we suggest additional studies are necessary to test to what extent the candidate genes reviewed above contribute to the observed heritabilities and genetic correlations. The extent that alleles in candidate genes explain heritable variation in the iris characteristics can readily be calculated with a slight modification of the structural equation model used in this study [55]. Iris data collected from twins may therefore provide a method to pinpoint how genes interact in the formation of different characteristics in the human iris.

ACKNOWLEDGEMENTS

This study was supported by funds from the Department of Social Sciences at Örebro University in Sweden and The Swedish Foundation for International Cooperation in Research and Higher Education. We are grateful to Dr. Angelica Burkhardt for preparing the data material, Anna Törnblom and Ulrika Sandberg for their accurate work as raters, and all the twins for their cooperation.

REFERENCES

1. Bito LZ, Matheny A, Cruickshanks KJ, Nondahl DM, Carino OB. Eye color changes past early childhood. The Louisville Twin Study. Arch Ophthalmol 1997; 115:659-63.
2. Larsson M, Pedersen NL, Stattin H. Importance of genetic effects for characteristics of the human iris. Twin Res 2003; 6:192-200.
3. Hsieh YW, Zhang XM, Lin E, Oliver G, Yang XJ. The homeobox gene Six3 is a potential regulator of anterior segment formation in the chick eye. Dev Biol 2002; 248:265-80.
4. Jaworski C, Sperbeck S, Graham C, Wistow G. Alternative splicing of Pax6 in bovine eye and evolutionary conservation of intron sequences. Biochem Biophys Res Commun 1997; 240:196-202.
5. Wentzel P, Bergh K, Wallin O, Niemela P, Stjernschantz J. Transcription of prostanoid receptor genes and cyclooxygenase enzyme genes in cultivated human iridial melanocytes from eyes of different colours. Pigment Cell Res 2003; 16:43-9.
6. Ragge NK, Falk RE, Cohen WE, Murphree AL. Images of Lisch nodules across the spectrum. Eye 1993; 7:95-101.
7. Kim I, Ryan AM, Rohan R, Amano S, Agular S, Miller JW, Adamis AP. Constitutive expression of VEGF, VEGFR-1, and VEGFR-2 in normal eyes. Invest Ophthalmol Vis Sci 1999; 40:2115-21. Erratum in: Invest Ophthalmol Vis Sci 2000; 41:368.
8. Kivela T, Jaaskelainen J, Vaheri A, Carpen O. Ezrin, a membrane-organizing protein, as a polarization marker of the retinal pigment epithelium in vertebrates. Cell Tissue Res 2000; 301:217-23.
9. Friedman JS, Faucher M, Hiscott P, Biron VL, Malenfant M, Turcotte P, Raymond V, Walter MA. Protein localization in the human eye and genetic screen of opticin. Hum Mol Genet 2002; 11:1333-42.
10. Smith RS, Zabaleta A, Kume T, Savinova OV, Kidson SH, Martin JE, Nishimura DY, Alward WL, Hogan BL, John SW. Haploinsufficiency of the transcription factors FOXC1 and FOXC2 results in aberrant ocular development. Hum Mol Genet

2000; 9:1021-32.
11. Huang W, Jaroszewski J, Ortego J, Escribano J, Coca-Prados M. Expression of the TIGR gene in the iris, ciliary body, and trabecular meshwork of the human eye. Ophthalmic Genet 2000; 21:155-69.
12. Kulak SC, Kozlowski K, Semina EV, Pearce WG, Walter MA. Mutation in the RIEG1 gene in patients with iridogoniodysgenesis syndrome. Hum Mol Genet 1998; 7:1113-7.
13. Orlow SJ, Brilliant MH. The pink-eyed dilution locus controls the biogenesis of melanosomes and levels of melanosomal proteins in the eye. Exp Eye Res 1999; 68:147-54.
14. Rebbeck TR, Kanetsky PA, Walker AH, Holmes R, Halpern AC, Schuchter LM, Elder DE, Guerry D. P gene as an inherited biomarker of human eye color. Cancer Epidemiol Biomarkers Prev 2002; 11:782-4.
15. Lichter PR, Richards JE, Downs CA, Stringham HM, Boehnke M, Farley FA. Cosegregation of open-angle glaucoma and the nail-patella syndrome. Am J Ophthalmol 1997; 124:506-15.
16. Pressman CL, Chen H, Johnson RL. LMX1B, a LIM homeodomain class transcription factor, is necessary for normal development of multiple tissues in the anterior segment of the murine eye. Genesis 2000; 26:15-25.
17. Monaghan AP, Davidson DR, Sime C, Graham E, Baldock R, Bhattacharya SS, Hill RE. The Msh-like homeobox genes define domains in the developing vertebrate eye. Development 1991; 112:1053-61.
18. Oetting WS, King RA. Molecular basis of albinism: mutations and polymorphisms of pigmentation genes associated with albinism. Hum Mutat 1999; 13:99-115.
19. Wistow G, Bernstein SL, Ray S, Wyatt MK, Behal A, Touchman JW, Bouffard G, Smith D, Peterson K. Expressed sequence tag analysis of adult human iris for the NEIBank Project: steroid-response factors and similarities with retinal pigment epithelium. Mol Vis 2002; 8:185-95 .
20. Simpson TI, Price DJ. Pax6; a pleiotropic player in development. Bioessays 2002; 24:1041-51.
21. Graw J. Genetic aspects of embryonic eye development in vertebrates. Dev Genet 1996; 18:181-97.
22. Sale MM, Craig JE, Charlesworth JC, FitzGerald LM, Hanson IM, Dickinson JL, Matthews SJ, Heyningen Vv V, Fingert JH, Mackey DA. Broad phenotypic variability in a single pedigree with a novel 1410delC mutation in the PST domain of the PAX6 gene. Hum Mutat 2002; 20:322.
23. Burkhardt A. [The color and structure of the human iris. 2. Studies of 200 twins]. Anthropol Anz 1992; 50:235-70.
24. Nichols RC, Bilbro WC Jr. The diagnosis of twin zygosity. Acta Genet Stat Med 1966; 16:265-75.
25. Kasriel J, Eaves L. The zygosity of twins: further evidence on the agreement between diagnosis by blood groups and written questionnaires. J Biosoc Sci 1976; 8:263-6.
26. Neale MC, Cardon LR. Methodology for genetic studies of twins and families. Kluwer Academic Publisher; 1992.
27. McGue M, Bouchard TJ Jr. Adjustment of twin data for the effects of age and sex. Behav Genet 1984; 14:325-43.
28. Neale MC, Walters EE, Eaves LJ, Maes HH, Kendler KS. Multivariate genetic analysis of twin-family data on fears: Mx models. Behav Genet 1994; 24:119-39.
29. Peck R, Williams LA. SPSS Manual. Boston: Addison Wesley Publishing Company; 2002.
30. Akaike H. Factor analysis and AIC. Psychometrika 1987; 52:317-32.
31. Eagle RC Jr. Iris pigmentation and pigmented lesions: an ultrastructural study. Trans Am Ophthalmol Soc 1988; 86:581-687.
32. Jakobiec FA, Silbert G. Are most iris “melanomas” really nevi? A clinicopathologic study of 189 lesions. Arch Ophthalmol 1981; 99:2117-32.
33. Oyster CW. The human eye: structure and function. Sunderland (MA): Sinauer Associates; 1999.
34. Imesch PD, Bindley CD, Khademian Z, Ladd B, Gangnon R, Albert DM, Wallow IH. Melanocytes and iris color. Electron microscopic findings. Arch Ophthalmol 1996; 114:443-7.
35. Donaldson DD. The significance of spotting of the iris in mongolids: Brushfield spots. Arch Ophthalmol 1961; 65:26-31.
36. Brooke Williams RD. Brushfield spots and Wolfflin nodules in the iris: an appraisal in handicapped children. Dev Med Child Neurol 1981; 23:646-9.
37. Opdecamp K, Nakayama A, Nguyen MT, Hodgkinson CA, Pavan WJ, Arnheiter H. Melanocyte development in vivo and in neural crest cell cultures: crucial dependence on the Mitf basic-helix-loop-helix-zipper transcription factor. Development 1997; 124:2377-86.
38. Yavuzer U, Keenan E, Lowings P, Vachtenheim J, Currie G, Goding CR. The Microphthalmia gene product interacts with the retinoblastoma protein in vitro and is a target for deregulation of melanocyte-specific transcription. Oncogene 1995; 10:123-34.
39. Planque N, Leconte L, Coquelle FM, Martin P, Saule S. Specific Pax-6/microphthalmia transcription factor interactions involve their DNA-binding domains and inhibit transcriptional properties of both proteins. J Biol Chem 2001; 276:29330-7.
40. Mochii M, Mazaki Y, Mizuno N, Hayashi H, Eguchi G. Role of Mitf in differentiation and transdifferentiation of chicken pigmented epithelial cell. Dev Biol 1998; 193:47-62.
41. Schedl A, Ross A, Lee M, Engelkamp D, Rashbass P, van Heyningen V, Hastie ND. Influence of PAX6 gene dosage on development: overexpression causes severe eye abnormalities. Cell 1996; 86:71-82.
42. Alward WL. Axenfeld-Rieger syndrome in the age of molecular genetics. Am J Ophthalmol 2000; 130:107-15.
43. Jaeger EA. Ocular findings in Down’s syndrome. Trans Am Ophthalmol Soc 1980; 78:808-45.
44. Purtscher E. [Nodular densification of stroma iridis in mongolism.]. Albrecht Von Graefes Arch Ophthalmol 1958; 160:200-15.
45. Lowe R. The eyes in mongolism. Br J Ophthalmol 1949; 33:131-54.
46. Delabar JM, Theophile D, Rahmani Z, Chettouh Z, Blouin JL, Prieur M, Noel B, Sinet PM. Molecular mapping of twenty-four features of Down syndrome on chromosome 21. Eur J Hum Genet 1993; 1:114-24.
47. Rao VN, Papas TS, Reddy ES. erg, a human ets-related gene on chromosome 21: alternative splicing, polyadenylation, and translation. Science 1987; 237:635-9.
48. Boulukos KE, Pognonec P, Begue A, Galibert F, Gesquiere JC, Stehelin D, Ghysdael J. Identification in chickens of an evolutionarily conserved cellular ets-2 gene (c-ets-2) encoding nuclear proteins related to the products of the c-ets proto-oncogene. EMBO J 1988; 7:697-705.
49. Landsman D, McBride OW, Soares N, Crippa MP, Srikantha T, Bustin M. Chromosomal protein HMG-14. Identification, characterization, and chromosome localization of a functional gene from the large human multigene family. J Biol Chem 1989; 264:3421-7.
50. Horisberger MA, Wathelet M, Szpirer J, Szpirer C, Islam Q, Levan G, Huez G, Content J. cDNA cloning and assignment to chro-

mosome 21 of IFI-78K gene, the human equivalent of murine Mx gene. Somat Cell Mol Genet 1988; 14:123-31.

51. Egeo A, Mazzocco M, Sotgia F, Arrigo P, Oliva R, Bergonon S, Nizetic D, Rasore-Quartino A, Scartezzini P. Identification and characterization of a new human cDNA from chromosome 21q22.3 encoding a basic nuclear protein. Hum Genet 1998; 102:289-93.
52. Fuentes JJ, Pritchard MA, Planas AM, Bosch A, Ferrer I, Estivill X. A new human gene from the Down syndrome critical region encodes a proline-rich protein highly expressed in fetal brain and heart. Hum Mol Genet 1995; 4:1935-44.
53. Vidal-Taboada JM, Bergonon S, Scartezzini P, Egeo A, Nizetic D, Oliva R. High-resolution physical map and identification of potentially regulatory sequences of the human SH3BGR located in the Down syndrome chromosomal region. Biochem Biophys Res Commun 1997; 241:321-6.
54. Gosset P, Crete N, Ait Ghezala G, Theophile D, Van Broeckhoven C, Vayssettes C, Sinet PM, Creau N. A high-resolution map of 1.6 Mb in the Down syndrome region: a new map between D21S55 and ETS2. Mamm Genome 1995; 6:127-30.
55. Zhu G, Duffy DL, Eldridge A, Grace M, Mayne C, O'Gorman L, Aitken JF, Neale MC, Hayward NK, Green AC, Martin NG. A major quantitative-trait locus for mole density is linked to the familial melanoma gene CDKN2A: a maximum-likelihood combined linkage and association analysis in twins and their sibs. Am J Hum Genet 1999; 65:483-92.

The print version of this article was created on 2 Nov 2004. This reflects all typographical corrections and errata to the article through that date. Details of any changes may be found in the online version of the article.